JOURNAL OF MATERIALS SCIENCE 31 (1996) 2325–2332

Thermal and photochemical methods for the preparation of thin films of cermet materials

G. LASSALETTA, A. R. GONZÁLEZ-ELIPE, A. JUSTO, A. FERNÁNDEZ*
Instituto de Ciencia de Materiales de Sevilla and Dpto. Química Inorgánica, CSIC-UNSE, P.O. Box 1115, 41080 Sevilla, Spain

F. J. AGER, M. A. RESPALDIZA
Facultad de Física, Universidad de Sevilla, P.O. Box 1065, 41080 Sevilla, Spain

J. C. SOARES
Centro de Física Nuclear, Universidade de Lisboa, Av. Prof. Gama Pinto 2, P-1699 Lisboa Cedex, Portugal

M. F. DA SILVA
Instituto Technologico e Nuclear, Departamento de Física-ICEN, Estrada Nacional 10, P-2685 Sacavem, Portugal

The synthesis of thin films of Ag–SiO_2, Ag–TiO_2 and Ag–TiO_2–SiO_2 cermet materials is described. The preparation method consists in a sol–gel process based in the dip-coating technique to obtain thin films of a composite material containing the oxidized metal and the corresponding ceramic material (TiO_2 and/or SiO_2). The films, prepared on quartz, were finally heated or irradiated to induce the reduction of the metal and the formation of the cermet materials. An exhaustive characterization of the samples has been carried out by scanning electron microscopy, X-ray diffraction, transmission electron microscopy, and Rutherford backscattering. The optical properties of the prepared thin films were determined by UV–VIS absorption spectroscopy and related to the microstructural characteristics of the cermet. Conclusions have been postulated to relate the experimental conditions of the synthesis (thermal or photochemical) to the microstructure and properties of the resulting materials.

1. Introduction

Small metal particles have been the subject of extensive investigations in recent years because of their interesting electrical [1] and optical [2] behaviour. These are essentially composites made of metal and a dielectric phase and are referred to as cermets (ceramic–metal) or discontinuous metal films. Electrical conductivity in these materials arises essentially due to an activated tunnelling of electrons between the metal islands [3]. In addition, effective medium theories predict that electrically disconnected metal particles, which are small relative to the wavelength of the impinging light, will be transparent [4–6]. So, electrically conductive and, at the same time, light-transparent materials can be prepared [7]. Another interesting property of nanosized metal particles embedded in a suitable matrix is the appearance in the optical absorption spectra of a surface plasma resonance peak [8, 9]. The absorption of light by such particles may be regarded as a plasma effect. The incident light polarizes the conduction electron gas of the metal spheres, producing an electric moment which oscillates with the frequency, w, of the light. When w approaches the natural frequency of the electron gas in the particle (the surface plasma frequency), a resonance absorption occurs [8, 9]. For this reason, metal (copper, silver, gold) particle-doped glasses are well known for their colour effect [10]. However, the third-order optical non-linearity of these materials is becoming an important area of research, and hence attracting renewed interest from the viewpoint of the fabrication of cermet materials [11].

Finally, it is interesting to mention that the strengthening and toughening of ceramic materials has been widely investigated through the years. The dispersion of a ductile metallic phase in a brittle ceramic matrix was found to be a promising method [12]. Reinforcement models show the importance of the microstructure of the ceramic–metal (cermet) composite materials.

Owing to the above-mentioned intriguing properties of cermet materials, renewed interest is being developed for their production. Melting and a subsequent growth by irradiation was one of the oldest

* Author to whom all correspondence should be addressed.

0022–2461

ways of developing metal-doped glasses [13]. Ion implantation and sputtering are being used widely to prepare various metal–ceramic films [14, 16]. Recently, the sol–gel process has been successfully employed to develop gold and copper-doped silica thin films on glass [11, 17]. Another approach to the problem consists in the synthesis of the desired material within the pores of a nanoporous membrane. This method has been called template synthesis [7], because the pores in the host membrane act as templates for the formation of nanostructures composed of the metallic particles [18, 19].

The present work investigated the synthesis of thin films of Ag–SiO_2, Ag–TiO_2 and Ag–TiO_2–SiO_2 cermet materials on quartz substrates by a sol–gel process combined with thermal and/or photochemical treatments to achieve the reduction of the metal. The two different ceramic matrices (TiO_2 and SiO_2) have been selected according to their different dielectric constants which, according to effective medium theories, should produce changes in the optical plasmon resonance characteristics of the cermet [20, 21]. On the other hand, titania appears to be a very interesting matrix due to the well-known photocatalytic activity [22, 23] of TiO_2 for the reduction of noble metals [24–28] which allows a room-temperature photochemical method to be used for the synthesis of the cermet materials.

A full characterization of the structure of the samples will be correlated with the optical characteristics of the materials.

2. Experimental procedure

Coatings were prepared on quartz slides by a dipping technique [29] using a motor-driven puller that lifts the quartz substrates at a constant rate (8 in. min^{-1}) from a solution containing the appropriate alcoxide precursor ($Ti(OCH(CH_3)_2)_4$ and/or $Si(OCH_2CH_3)_4$) and the silver salt ($AgNO_3$). Several samples have been prepared depending on the composition of the precursor solution as summarized in Table I. These solutions correspond to an atomic ratio Ag/Ti, Ag/Si or Ag/(Ti + Si) of 1/6 in all the preparations. After lifting, the samples were dried in air for 2 h so that the hydrolysis of the alcoholate occurs by reaction with ambient moisture [29]. Finally, the samples were calcined either at 373 or at 673 K for 2 h to achieve the full formation of the ceramic matrix (SiO_2 and/or TiO_2).

The photochemical reduction of the silver phase in the thin films was carried out by illumination of the samples in air using an irradiation system from Oriel which consisted of a power supply, a Hg–Xe 500 W lamp, a water filter for elimination of infrared radiation and an optical fibre system made of quartz for driving the light at the top of the slides. The samples were illuminated for the same time on both sides.

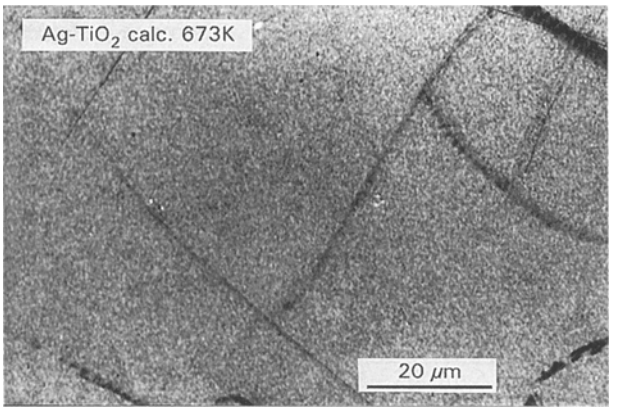

Figure 1 Scanning electron micrograph obtained for the Ag–TiO_2 sample after heating in air at 673 K.

The scanning electron micrographs were obtained on a Jeol JSM5400 microscope working at 20 kV and implemented with an energy dispersive spectroscopy accessory (EDX).

Fig. 1 presents the SEM analysis of the Ag–TiO_2 sample calcined at 673 K showing the general texture and morphology obtained for the films which, in general, are homogeneous and compact. In the scanning electron microscope we have also measured by EDX the TiK_α fluorescence signal for this sample and for a pressed pellet of TiO_2 Degussa P-25 used as reference. From these measurements and according to the method given by Waldo *et al.* [30], we have evaluated a thickness for the Ag–TiO_2 thin film of ~ 100 nm. All the prepared thin films have thicknesses around that value, in agreement with RBS measurements, as we will show later.

X-ray diffraction analysis (XRD) was carried out using CuK_α radiation in a Siemens D5000 diffractometer provided with a thin-film attachment (0.4° Soller slit and LiF (1 0 0) monochromator in the detector arm). To take the diagrams, typical incident angles of 0.5° were used.

UV–VIS absorption spectra were recorded in a Shimadzu UV-2101 PC instrument in the transmission mode.

For the transmission electron microscopy, the thin films were scraped out from the coated substrates with a diamond pencil and the obtained powder was dispersed in ethanol and dropped on a conventional

TABLE I Composition of the precursor solution for the synthesis of the different thin-film samples

Sample	i-PrOH (ml)	$AgNO_3$ (g)	$Ti(OCH(CH_3)_2)_4$ (ml)	$Si(OC_2H_5)_4$ (ml)
Ag–TiO_2	40	0.3	3.2	–
Ag–SiO_2	40	0.3	–	2.4
Ag–TiO_2(5)–SiO_2	40	0.3	0.1	2.3
Ag–TiO_2(50)–SiO_2	40	0.3	1.6	1.2

carbon-coated copper grid. The micrographs were obtained in a Hitachi H800 microscope working at 200 kV.

X-ray photoelectron spectra were recorded with a VG Escalab 220 using the MgK_α excitation source and working in the pass energy constant mode at 50 eV. Calibration of the spectra was done at the C1s peak of surface contamination taken at 284.6 eV.

The thickness and the homogeneity in depth of the silver and titanium contents of the samples have been studied by using Rutherford Backscattering (RBS) analysis. This technique is quite appropriate for the range of thicknesses of the films studied. In addition, the technique appears to be very convenient in comparison to X-ray photoelectron spectroscopy (XPS) sputtering depth profiling analysis, which is limited by preferential sputtering effects and phase mixing induced by ion bombardment. The RBS analysis also has higher depth resolution and allows very small changes in the depth profiles of the silver and titanium elements to be observed. RBS analyses were performed on the 3 MV Van de Graaff accelerator at the Instituto Technológico e Nuclear, Sacavém, Portugal, using 1 MeV alpha particles. The incident beam, normal to the sample surface or tilted 30° (to increase depth resolution by increasing the path traversed by the particles), was collimated up to 1 mm diameter. Backscattered alphas were detected either at 140° or at near 180° with an annular detector. The spectra were analysed using the RUMP computer program [31]. To avoid the incidence of the luminiscent light emmitted by the quartz substrate into the detectors, low beam intensities and a mask to cover the samples were used.

3. Results and discussion

3.1. Thermal reduction of the silver phase in the cermet thin films

In the first part of this work we have studied the effect of calcination at 673 K of the different samples after preparation by dip coating and subsequent drying in air at room temperature for 2 h. This treatment produces the total decomposition of the alcoxide precursors to yield the SiO_2 and TiO_2 phases. Fig. 2 shows

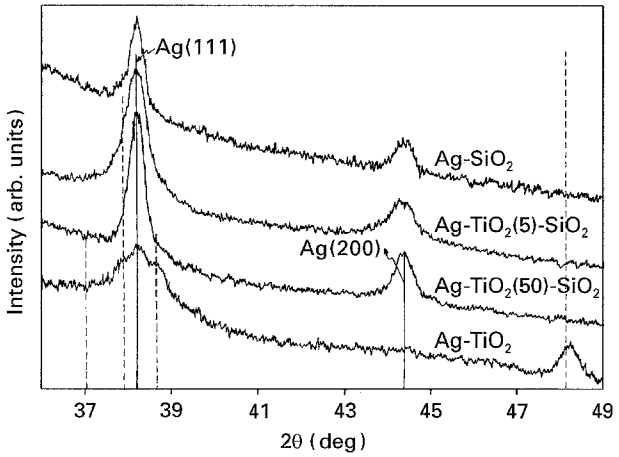

Figure 2 XRD diffraction pattern obtained for the silver–oxide cermet materials after heating in air at 673 K. (——) Metallic silver peaks, (– – –) anatase TiO_2 peaks.

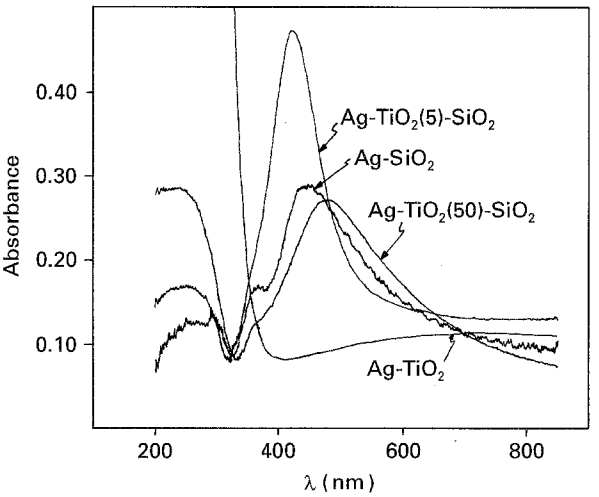

Figure 3 UV–VIS absorption spectra for the silver–oxide cermet materials after heating in air at 673 K.

the XRD patterns obtained for the different samples after this calcination at 673 K. In this figure it is clearly observed that in samples Ag–SiO_2, Ag–TiO_2(5)–SiO_2 and Ag–TiO_2(50)–SiO_2 the silver phase has been reduced, forming crystallites of small size as indicated by the silver 1 1 1 and 2 0 0 diffraction peaks detected by XRD. This thermal reduction is in agreement with the well-known decomposition of the silver oxide to yield reduced silver [32]. On the other hand, the TiO_2 phase in the Ag–TiO_2 sample also shows a certain degree of crystallization (see Fig. 2); however, in this sample it appears that a metallic silver phase is not well formed. As we will discuss later, this must be due to the stabilization in this sample of the Ag^+ state of silver dispersed through the TiO_2 phase.

An important characteristic of these thin films supported on quartz is their UV–VIS absorption behaviour. The spectra are depicted in Fig. 3 where we can detect an important plasmon resonance absorption band with a maximum between 420 and 480 nm for the samples Ag–SiO_2 (λ_{max} = 442 nm), Ag–TiO_2(5)–SiO_2 (λ_{max} = 426 nm) and Ag–TiO_2(50)–SiO_2 (λ_{max} = 482 nm) while again the Ag–TiO_2 sample shows the absence of such an intense absorption peak at these photon energies. The absence of such a feature in the optical absorption spectra of the thermally treated Ag–TiO_2 sample indicates the absence of small metallic silver particles in this sample and, as a consequence, that the cermet material cannot be formed by annealing in air.

On the other hand, the TEM analysis of the samples exhibiting plasma resonance in the UV–VIS absorption spectra shows effectively the presence of small silver particles (see Fig. 4, as an example). Particle-size distribution curves have been evaluated from numerous micrographs and the results are depicted in Fig. 5. Particle sizes ranging from 2–10, 2–25 and 3–20 nm have been determined for the samples Ag–SiO_2, Ag–TiO_2(5)–SiO_2 and Ag–TiO_2(50)–SiO_2, respectively.

In summary, the small XRD diffraction peaks, as well as the absence of a plasmon absorption band for the thermally treated Ag–TiO_2 sample, are important evidence that in this sample the silver phase is not

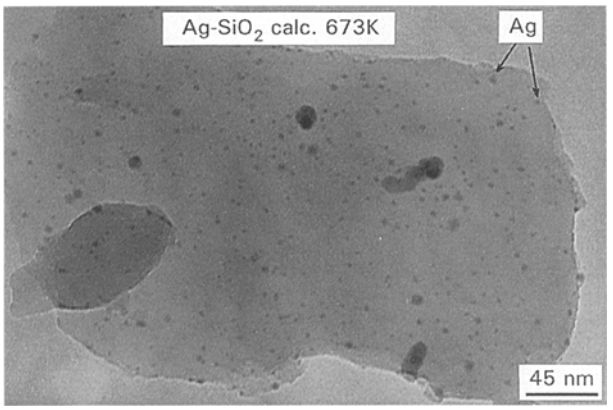

Figure 4 Transmission electron micrograph obtained for the $Ag–SiO_2$ sample after heating in air at 673 K.

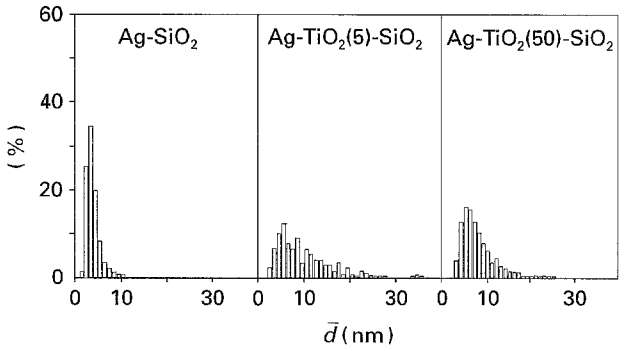

Figure 5 Particle-size distribution of the silver phase obtained by TEM for the silver–oxide cermet materials after heating in air at 673 K.

reduced, remaining as Ag^+ in a highly dispersed phase through the TiO_2 matrix. This conclusion has been confirmed by XPS by monitoring the Ag*M N N* Auger peak which shows the presence of oxidized Ag^+ species in this sample. All other cermets ($Ag–SiO_2$ and $Ag–TiO_2–SiO_2$) could be prepared by thermal reduction of the metallic phase. At this point we decided to test a photochemical method to induce the reduction of silver and the formation of the desired cermet thin film in the case of $Ag–TiO_2$ on the basis of the well-known photocatalytic activity [22, 23] of the TiO_2 for the photoreduction of noble metals [24–28]. This method will be described in the next section.

3.2. Photochemical reduction of the silver phase in the $Ag–TiO_2$ sample

Fig. 6 shows the UV–VIS absorption spectra for the $Ag–TiO_2$ sample after calcination at 673 K and subsequent illumination for different times. From the figure it can be seen that a broad plasmon with an absorption which extends to long wavelengths has evolved. This UV–VIS absorption behaviour is accompained by the evolution of the characteristic diffraction peaks for silver in the X-ray diffractograms, as shown in Fig. 7. Both effects indicate the formation of reduced silver; thus showing that a photochemical method can be used for the preparation of the $Ag–TiO_2$ cermet films that could not be prepared by thermal reduction.

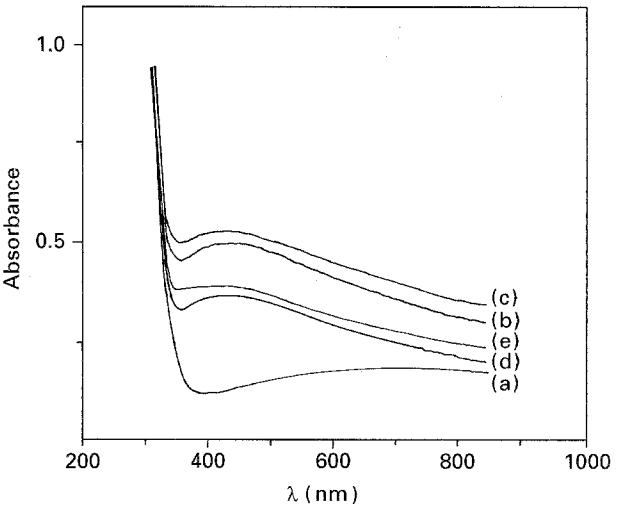

Figure 6 UV–VIS absorption spectra for $Ag–TiO_2$ sample after calcination at 673 K and subsequent illumination for different times: (a) 0 min, (b) 15 min, (c) 30 min, (d) 45 min, (e) 105 min.

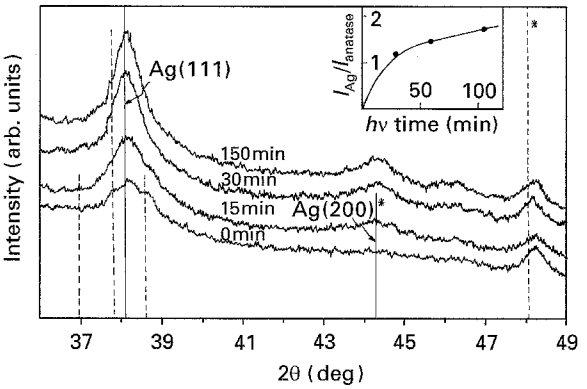

Figure 7 XRD diffraction pattern obtained for the $Ag–TiO_2$ sample after calcination at 673 K and subsequent illumination for different times. (——) Metallic silver peaks, (– – –) anatase TiO_2 peaks. Inset: intensity of the Ag(200) peak relative to the anatase intensity as a function of the illumination time.

However, the $Ag–TiO_2$ cermet prepared under illumination presents a broad plasmon and an optical absorption which extend to high wavelengths. This indicates the formation of an heterogeneous distribution of silver particles and even the interconnection of the particles leading to a bulk metal-like behaviour in the UV–VIS absorption spectra. In fact, the transmission electron micrograph in Fig. 8 shows the appearance of silver aggregates, thus indicating a high rate of reduction of silver as is usually observed for the photoreduction of this metal on titania [33, 34]. In addition, RBS analysis of a $Ag–TiO_2$ sample was carried out. A typical RBS spectrum and its simulation are shown in Fig. 9, including the depth scale for silver and titanium peaks obtained from the results of the RUMP simulations discussed below. These results obtained with the sample after calcination at 673 K and subsequent illumination have been summarized in Fig. 10. Titanium and silver profiles obtained after simulations of the sample structure, show a homogeneous film with silver distributed along the TiO_2 layer corresponding to the formation of the desired cermet material. Assuming the atomic density of the

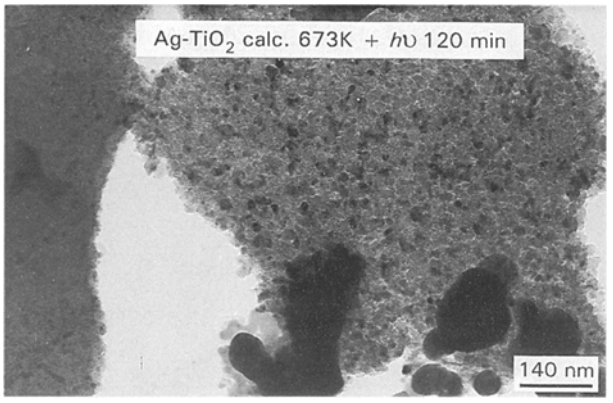

Figure 8 Transmission electron micrograph obtained for the Ag–TiO_2 sample after calcination at 673 K and subsequent illumination for 120 min.

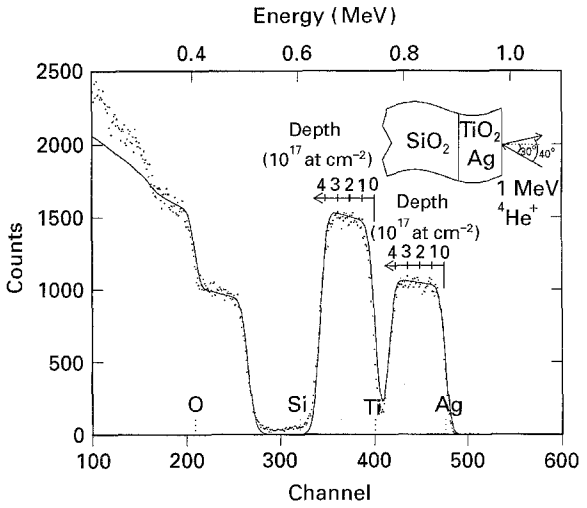

Figure 9 RBS spectrum for (···) the Ag–TiO_2 sample (calcination at 673 K, $h\upsilon = 0$ min) showing the titanium and silicon peaks and the silica substrate. The depth scale provided by the RUMP program is also included (——).

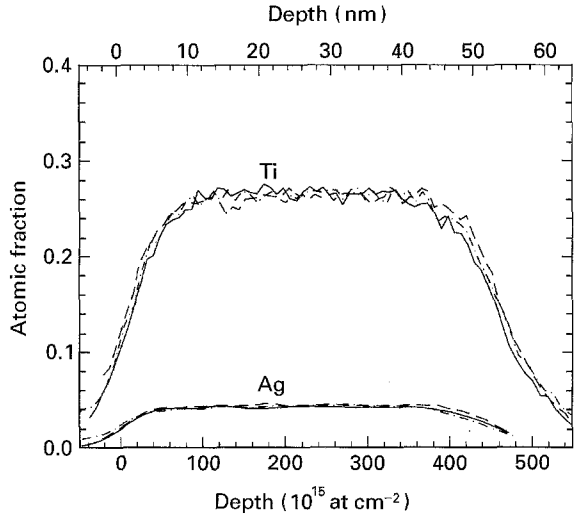

Figure 10 RBS titanium and silver profiles obtained for the Ag–TiO_2 sample after calcination at 673 K and subsequent illumination for different times: (——) 0 min, (– – –) 40 min, (–·–) 60 min.

layer to be mainly that of TiO_2-anatase, that is, 8.68 at cm^{-3}, we can convert the areal density on the bottom axis in Fig. 10, natural RBS units, to the distance units on the top axis.

It should be mentioned here that after calcination at 673 K the Ag–SiO_2, Ag–TiO_2(5)–SiO_2 and Ag–TiO_2(50)–SiO_2 samples appeared stable against illumination, so that no changes in the UV–VIS absorption plasmon were observed. However, if the samples are heated in air after their preparation just at 373 K, the reduction of the silver phase can be carried out photochemically. This process will be described below.

3.3. Photochemical reduction of the silver phase in the Ag–SiO_2 and Ag–TiO_2–SiO_2 samples

When the Ag–SiO_2, Ag–TiO_2(5)–SiO_2 and Ag–TiO_2(50)–SiO_2 are heated in air at 373 K, their subsequent illumination produces the growth of a plasmon resonance in their optical absorption spectra, as represented in Fig. 11. This effect must correspond to the photochemical reduction of silver under these experimental conditions. It should be emphasized here that the plasmon resonance initially present in the samples before illumination is always smaller for the sample containing a higher amount of TiO_2, a feature that indicates that the thermal reduction of silver in the titania matrix is less efficient than the photochemically assisted procedure.

As an example of the growth of the silver crystallites under illumination, we have included in Fig. 12 the XRD diffraction patterns for the Ag–SiO_2 sample after different irradiation times. The formation of silver particles can be also followed by TEM, where we could obtain from numerous micrographs particle size-distribution curves. Two of these curves are included in Fig. 13; in comparison with Fig. 5 it is possible to conclude that a higher agglomeration and a higher size heterogeneity of the silver particles is induced under illumination in comparison to the thermal reduction process. Particle sizes ranging from 2–40 and 3–70 nm have been determined for the

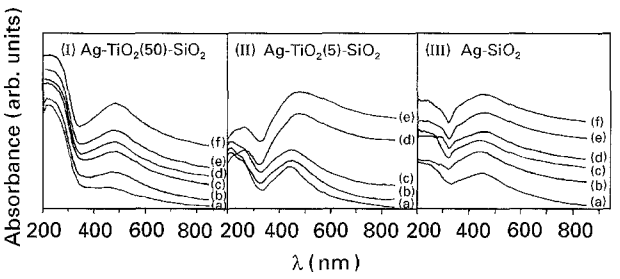

Figure 11 UV–VIS absorption spectra obtained for the different silver–oxide cermet materials after heating in air at 373 K and subsequent illumination for increasing periods of time: (I) (a) 0 min to (f) 90 min., (II) (a) 0 min to (e) 60 min, (III) (a) 0 min to (f) 135 min.

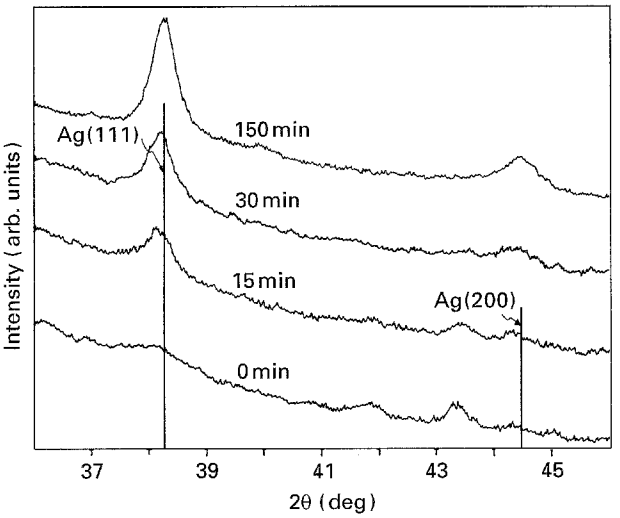

Figure 12 XRD diffraction pattern obtained for the Ag–SiO_2 sample after heating in air at 373 K and subsequent illumination for increasing periods of time.

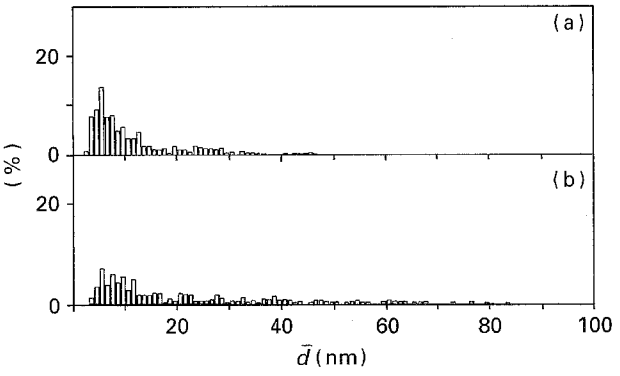

Figure 13 Particle-size distribution of the silver phase obtained by TEM for (a) the Ag–SiO_2 and (b) Ag–TiO_2 (50)–SiO_2 cermet thin films after heating in air at 373 K and subsequent illumination: (a) 150 min, (b) 90 min.

Ag–SiO_2 and Ag–TiO_2(50)–SiO_2 samples, respectively. This broad size distribution should produce a broad plasmon in the UV–VIS absorption spectra, as is actually observed in Fig. 11.

It is also important to mention that the sample with a higher titania content (i.e. Ag–TiO_2(50)–SiO_2) has also a particle-size distribution curve which extends to very high diameters, this is due to the agglomeration effect which, as shown for the irradiated Ag–TiO_2 sample, is especially promoted by TiO_2. In fact, for the Ag–TiO_2 sample, the interconnection of the particles was so high that it was not possible to distinguish clearly the limit of each particle.

Fig. 14 shows the RBS titanium and silver profiles for different Ag–TiO_2(50)–SiO_2 samples subjected to heating in air at 373 and 673 K and subsequent illumination. Unlike in Fig. 10, where the analyses were carried out on the same sample, for comparison in this case the depth scale has been normalized, because different samples have slightly different thicknesses. Again we observe an homogeneous distribution of silver along the TiO_2 layer which corresponds to the formation of a homogeneous cermet thin film.

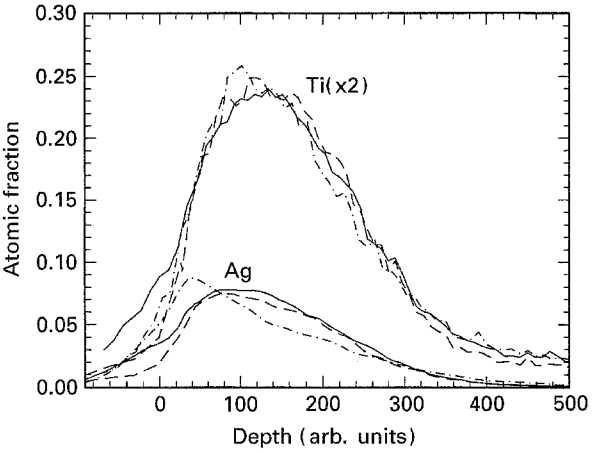

Figure 14 RBS titanium and silver profiles obtained for different Ag–TiO_2(50)–SiO_2 samples subjected to calcination at (——) 373 and (– · –) 673 K and (– – –) also after illumination in air for 60 min. For comparison, the depth scales have been normalized.

Finally it is interesting to mention that two different mechanisms should opperate during the photochemical synthesis of the cermet thin films. In the case of a Ag–SiO_2 sample the photoreduction of silver may occur via the light-induced decomposition of silver oxides which can occur even at 298 K [32]. However, in the case of titania-containing samples, a new mechanism is possible due to the photoactivity of TiO_2 for the reduction of noble metals. Titania is a semiconductor, so that band-gap illumination generates electron-hole pairs according to

$$TiO_2 \xrightarrow{h\nu} TiO_2(h^+_{VB}, e^-_{CB}) \quad (1)$$

Then, the reduction of silver cations by the semiconductor free electrons into zerovalent metal atoms must occur, i.e.

$$Ag^+ + e^-_{CB} \rightarrow Ag^0 \quad (2)$$

a process that is accompanied by the oxidation of OH groups or organic contaminants at the surface of TiO_2 by the holes at the valence band. This photoreduction of metal atoms, catalysed by the titania semiconductor, is a well-known process [24–28] and allows a new and very efficient route for the photoreduction of silver. The fast kinetics induced by the presence of the semiconductor in comparison with pure silica may account for the differences between both types of samples.

3.4. Analysis of the optical absorption spectra

The Mie theory [35] for surface plasma resonance in small metallic particles can explain, at least qualitatively, the optical absorption spectra of the cermet thin films. The spectra of metal colloids with particles in the size range of 3–20 nm are determined to a good approximation by only the dipole term in the Mie series. According to this approximation the absorption cross-section for a spherical particle of volume, V, is given by [35]

$$G = 18\pi V\varepsilon_2/\lambda[(\varepsilon_1 + 2)^2 + \varepsilon_2^2] \quad (3)$$

where λ is the wavelength in the surrounding medium, and $\varepsilon_1 + i\varepsilon_2 = \varepsilon$ is the complex relative permittivity of the metal relative to that of the surrounding medium. Generally, the theory predicts and experiment confirms that, as the dielectric constant of the host medium increases, the wavelength at the maximum of the plasma, λ_{max}, shifts to lower energy and the absorption band broadens. This is what we observe in Figs 3 and 11, because the absorption maximum is shifted to higher wavelengths for the samples with higher titania contents (higher dielectric constant of TiO_2 in comparison to SiO_2).

In addition, the Mie theory predicts that for very small particles, both λ_{max} and $\Delta w_{1/2}$ (band width) are independent of particle size, because Equation 3 is independent of R. This behaviour is generally not observed [36–38]. In a classical manner, a size dependence can be introduced by supposing that the dielectric constant for the particle depends on the particle radius. The result [8] is the following inverse dependence of the bandwidth on the particle radius

$$\Delta w_{1/2} = V_F/R \quad (4)$$

where V_F is the Fermi velocity. This relationship has been verified by a number of researchers [36–40] and corresponds to that effect observed in this paper, so that in Fig. 3 the broader peaks correspond to the Ag–SiO_2 and Ag–TiO_2(50)–SiO_2 samples with smaller mean particle size (see Fig. 5).

The Mie theory is, however, a very simple model than can be applied for isolated particles; for metal-concentrated samples when the metal particles occupy an important volume fraction of the surrounding medium, the application of the Maxwell–Garnett theory or one of the effective medium theories [20, 21] is required. In particular, the high heterogeneity in the size-distribution curves and the high connectivity of the metallic particles detected in the Ag–TiO_2 sample must be the origin of the important broadening of the plasma resonance peak in this sample (see Fig. 6).

4. Conclusions

The synthesis of thin films of Ag–SiO_2, Ag–TiO_2 and Ag–TiO_2–SiO_2 cermet materials was investigated. As a consequence of the different experimental procedures (thermal or photochemical) for the reduction of silver, different cermet (silver–oxide) materials can be synthesized. The optical characteristics of such thin layers are different according to the different preparation procedures. We can summarize the characteristics of the samples obtained under the different experimental conditions as follows.

1. Ag–SiO_2 and Ag–TiO_2–SiO_2 cermets could be prepared by thermal reduction (calcination at 673 K) of silver. The resulting materials had well-defined silver particles embedded in the ceramic matrix with a narrow particle-size distribution. This is accompanied by the appearance of a well-defined and narrow absorption peak in the UV-VIS spectrum that corresponds to the appearance of characteristic colours in the samples.

2. The photochemical reduction of silver in the Ag–SiO_2 and Ag–TiO_2–SiO_2 cermets thin films always leads to the formation of a cermet with a broad particle-size distribution that corresponds to a broader plasmon absorption peak in comparison with the thermally prepared cermet.

3. The Ag–TiO_2 cermet should be synthesized by a photochemical reduction due to the fact that in the thermally treated sample, silver is stabilized in an oxidized state in the titania matrix. The resulting cermet presents a broad particle-size distribution of the metallic phase with interconnection of the silver particles that corresponds to a very broad plasmon absorption extended to high wavelengths.

Acknowledgements

The authors thank the DGICYT (Project PB93-0183) for financial support. The facilities provided by the "Servicio de Microscopía Electrónica de la Universidad de Sevilla" are also acknowledged.

References

1. B. ABELES, S. PING, M. D. COUTTS and Y. ARIE, *Adv. Phys.* **24** (1975) 407.
2. C. A. NIKLASSON, C. G. GRANQVIST and O. HUNDERI, *Appl. Opt.* **30** (1981) 26.
3. C. A. NEUGEBAUER and M. B. WEBB, *J. Appl. Phys.* **33** (1962) 74.
4. D. E. ASPNES, *Thin Solid Films* **89** (1982) 249.
5. A. HELLER, D. E. ASPNES, J. D. PORTER, T. T. SHENG and R. G. VADIMSKY, *J. Phys. Chem.* **89** (1985) 4444.
6. D. E. ASPNES, A. HELLER and J. D. PORTER, *J. Appl. Phys.* **60** (1986) 3028.
7. C. A. FOSS Jr, G. L. HORNYAK, J. A. STOCKERT and C. R. MARTIN, *Adv. Mater.* **5** (1993) 135.
8. M. P. ANDREWS and G. A. OZIN, *J. Phys. Chem.* **90** (1986) 2929.
9. J. P. WILCOXON, R. L. WILLIAMSON and R. BAUGHMAN, *J. Chem. Phys.* **98** (1993) 9933.
10. C. R. BAMFORD, "Color Generation and Control in Glass" (Elsevier, New York, 1977).
11. D. KUNDU, J. HONNA, T. OSAWA and H. KOMIYAMA, *J. Am. Ceram. Soc.* 77 (1994) 1110.
12. A. G. EVANS, *Mater. Sci. Eng.* **A105/106** (1988) 65.
13. R. H. DOREMUS, *J. Chem. Phys.* **40** (1964) 2389.
14. H. HASONO, H. FUKUSHIMA, Y. ABE, R. A. WEEKS and R. A. ZHUR, *J. Non-Cryst. Solids* **143** (1982) 157.
15. K. FUKUMI, A. CHAYAHARA, K. KADONO, T. SAKAGUCHI, Y. HIRONO, M. MIYA, S. HAYAKAWA and M. SATOU, *Jpn J. Appl. Phys.* **30** (1991) L742.
16. T. AKAI, K. KADONO, H. YAMANAKA, T. SAKAGUCHI, M. MIYA and H. WAKABAYASHI, *J. Jpn. Ceram. Soc.* **101** (1993) 105.
17. J. MATSUOKA, R. MIZUTANI, S. KANEKO, H. NASU, K. KAMIYA, K. KADONO, T. SAKAGUCHI and M. MIYA, *ibid.* **101** (1993) 53.
18. M. J. THIERNEY and C. R. MARTIN, *J. Phys. Chem.* **93** (1989) 2878.
19. C. A. FOSS Jr, G. L. HORNYAK, J. A. STOCKERT and C. R. MARTIN, *ibid.* **96** (1992) 7497.
20. C. G. GRANQVIST, *J. Phys. C1* **42** (1981) 247.
21. S. BERTHIER, K. D. KHODJA and J. PEIRO, *Nanostruct. Mater.* **2** (1993) 421.
22. M. GRÄTZEL (ed.), "Energy Resources through Photochemistry and Catalysis" (Academic Press, New York, 1983).
23. A. HARRIMAN and M. A. WEST (eds.), "Photogeneration of Hydrogen" (Academic Press, London, 1982).
24. B. KRAUETLER and A. J. BARD, *J. Am. Chem. Soc.* **100** (1978) 4317.

25. K. H. STADLER and H. P. BOEHM, in "Proceedings of the 8th International Congress on Catalysis", Berlin, Vol. 4 (Verlag Chemie, Weinheim, 1984) p. 803.
26. J. M. HERRMANN, J. DISDIER, P. PICHAT, A. FERNÁNDEZ, A. R. GONZÁLEZ-ELIPE, G. MUNUERA and C. LECLERCQ, *J. Catal.* **132** (1991) 490.
27. A. FERNÁNDEZ and A. R. GONZÁLEZ-ELIPE, *Appl. Surf. Sci.* **69** (1993) 285.
28. E. BORGARELLO, N. SEPONE, G. EMO, R. HARRIS, E. PELIZZETTI and C. MINERO, *Inorg. Chem.* **25** (1986) 4499.
29. H. K. PULKER, in "Thin Films Science and Technology, "Vol. 6, "Coatings on Glass", edited by G. Siddall (Elsevier, Amsterdam, 1984) p. 109.
30. R. A. WALDO, M. C. MILITELLO and S. W. GAARENSTROOM, *Surf. Int. Anal.* **20** (1993) 111.
31. L. R. DOOLITTLE, *Nucl. Instr. Meth.* **B9** (1985) 344.
32. J. C. BAILAR, H. J. EMELÉUS, R. NYHOLM and A. F. TROTMAN-DICKENSON (eds), "Comprehensive Inorganic Chemistry" (Pergamon Press, Oxford, 1973).
33. J. M. HERRMANN, J. DISDIER and P. PICHAT, *J. Catal.* **113** (1988) 72.
34. H. HADA, Y. YONEZAWA and Y. MOMOKI, *Bull. Chem. Soc. Jpn.* **55** (1982) 3633.
35. M. KERKER, "The Scattering of Light and Other Electromagnetic Radiation" (Academic Press, New York, 1969) p. 38.
36. R. F. MARZKE, *Catal. Rev. Sci. Eng.* **19** (1979) 43.
37. M. DIGNAM and M. MOSKOVITS, *J. Chem. Soc. Farad. Trans. 2* **69** (1973) 65.
38. A. E. HUGHES and S. C. JAIN, *Adv. Phys.* **28** (1979) 717.
39. H. ABE, W. SCHULZE and B. TESCHE, *Chem. Phys.* **47** (1980) 95.
40. L. GENZEL, T. P. MARTIN and V. KREIBIG, *Z. Phys.* **21** (1975) 339.

Received 22 May
and accepted 20 November 1995